Molecular Immunology 116 (2019) 56–62

Contents lists available at ScienceDirect

Molecular Immunology

journal homepage: www.elsevier.com/locate/molimm

Bisperoxovanadium induces M2-type macrophages and promotes functional recovery after spinal cord injury

Jia Liu[a,1], Kai Li[b,1], Jing Zhou[c,1], Tian Sun[d], Chengliang Yang[a], Jihua Wei[a], Kegong Xie[a], Qisheng Luo[e,*], Yujin Tang[a,*]

[a] Department of Orthopedics, Affiliated Hospital of Youjiang Medical University for Nationalities, Baise, Guangxi, China
[b] Academy of Orthopedics, The Third Affiliated Hospital of Southern Medical University, Guangzhou, Guangdong, China
[c] Department of Anatomy, Affiliated Hospital of Youjiang Medical University for Nationalities, Baise, Guangxi, China
[d] Department of Orthopedic Spinal Surgery, Nanfang Hospital, Southern Medical University, Guangzhou, China
[e] Department of Neurosurgery, Affiliated Hospital of Youjiang Medical University for Nationalities, Baise, Guangxi, China

ARTICLE INFO

Keywords:
Bisperoxovanadium
M2-type macrophages
Acellular spinal cord
Spinal cord injury
PTEN

ABSTRACT

Macrophages can be polarized towards either a classically activated pro-inflammatory (M1) state, or alternatively towards an activated anti-inflammatory (M2) state. M1 cells are activated by ligands of toll-like receptor (TLR) or interferon (IFN)-γ and have a toxic effect, whereas M2 cells are activated by interleukin (IL)-4, IL-10, and IL-13 and have a regenerative effect in vitro and in vivo. Previously studies have shown that these cells play an important role in the inflammatory responses following spinal cord injury (SCI). Mechanistically, the role of PTEN in the regulation of macrophage polarization has yet to be fully elucidated. In the present study, we first evaluated the expression of PTEN in macrophages after SCI. We found that PTEN expression was accumulated in the macrophages after the SCI surgery. Knock-down of PTEN or inhibition of phospho-PTEN with bpV(pic) in RAW264.7 cells resulted in increased M2 polarization and decreased M1 polarization. In a rat model of SCI, grafts containing bpV(pic) reduced spinal tissue cavitation and promoted locomotor improvement, while combining grafts of bpV(pic) and acellular spinal cord (ASC) scaffolds showed a better effect. Moreover, grafts containing bpV(pic) enhanced M2 polarization and decreased M1 polarization in the macrophages during SCI. Thus, we have established that PTEN is critical for the polarization of macrophages and the functional recovery of SCI. Targeting PTEN enhances the macrophages towards to M2 polarization and promoting the functional recovery in SCI, and this suggest that PTEN may be a future therapeutic target for SCI treatment.

1. Introduction

Spinal cord injury (SCI) results in profound motor, sensory and autonomic impairments, which are associated with functional limitations, reduced participation in daily activities, and altered quality of life (Kirshblum et al., 2011). The rehabilitation of individuals with spinal cord injury (SCI) can be divided into three distinct phases: acute, subacute and chronic (Burns et al., 2017). The acute and subacute periods, when combined, generally correspond with the natural history of neuro-recovery, while the chronic phase is the period when neuro-recovery has plateaued.(Burns et al., 2017; Fawcett et al., 2007). Rehabilitation during the acute and subacute phases focuses on preventing secondary complications, promoting and enhancing neuro-recovery, maximizing function, and establishing optimal conditions for long-term maintenance of health and function (Halsey et al., 2018).

In the acute phase of spinal cord injury (SCI), inflammatory cells such as macrophages accumulate at the injured lesion following initial mechanical trauma to the spinal cord and release a variety of cytokines (David and Kroner, 2011; Fleming et al., 2006). Shortly after SCI injury, blood monocytes migrate to the site of injury, where they then differentiate into macrophages and play an important role in tissue repair (Allison and Ditor, 2015; Franken et al., 2016; Shechter et al., 2009). Two major subsets of macrophages can be distinguished based on their molecular phenotype and function: classically activated pro-inflammatory (M1) cells, and alternatively activated anti-inflammatory (M2) cells (Cambier et al., 2014; Kigerl et al., 2009; Liu and Yang, 2013; Pieters, 2008; Shapouri-Moghaddam et al., 2018). M1 macrophages express tumor necrosis factor alpha (TNF-a) and inducible nitric oxide

* Corresponding authors at: Hospital of Youjiang Medical University for Nationalities, 18 Zhongshan II Road, Baise, Guangxi, 533000, China.
E-mail addresses: 850198155@qq.com (Q. Luo), tangyujin1967@l63.com (Y. Tang).
[1] Jia Liu, Kai Li and Jing Zhou contributed equally to this study.

https://doi.org/10.1016/j.molimm.2019.09.022
Received 25 June 2019; Received in revised form 25 September 2019; Accepted 29 September 2019
Available online 09 October 2019

synthase (iNOS), and have proteolytic activity. M2 macrophages possess immune modulatory, phagocytic, tissue repair, and remodeling properties and express unique molecular markers such as arginase-1 and CD206 (Benoit et al., 2008; Ding et al., 2019; Mosser and Edwards, 2008; Stout and Suttles, 2004). Previous studies have shown that both M1 and M2 macrophages are present in the injured spinal cord, and that the spinal cord environment favors polarization towards a predominantly M1 cytotoxic macrophage phenotype (Gensel and Zhang, 2015; Wang et al., 2015). A few groups have reported that M1 macrophages are neurotoxic, whereas M2 macrophages promote axonal regeneration after central nervous system (CNS) injury (Ji et al., 2015; Li et al., 2015, 2016; Ma et al., 2015; Yao et al., 2014; Zhang et al., 2014). Thus, increasing the M2 cell population and promoting the presence of this macrophage subtype at the site of injury may be a promising strategy for tissue repair after SCI (Kong and Gao, 2017). In addition, the molecular mechanisms underlying the M2 transformation, and its effect on injured tissues, requires further investigation.

In this study, we observed that PTEN expression accumulated in macrophages after SCI in rats. Knockdown of PTEN in the cultured macrophage cell line RAW264.7 resulted in a transition towards a predominantly anti-inflammatory M2 macrophage phenotype. We then generated acellular spinal cord (ASC) scaffolds combined with the PTEN inhibitor bpV(pic), and transplanted these into spinal cord-injured rats. BpV(pic) in combination with an ASC reduced motor neurons loss and improved functional recovery after SCI (Tang et al., 2019). The macrophages in the injury site following SCI were polarized towards an M2 phenotype, rather than an M1 type, following grafting with bpV(pic) or an ASC combined with bpV(pic). Thus, we speculate that the neuronal protective effect of bpV(pic) after SCI occurs by promoting the polarization of macrophages towards an M2 phenotype.

2. Results

2.1. PTEN expression accumulates in macrophages after SCI

As previously reported, we observed via western blot analysis that the expression of PTEN was gradually increased in spinal cords after SCI (Fig. 1A, B). To examine whether this enhanced PTEN expression was present specifically in macrophages after SCI, we labeled macrophages with an anti-F4/80 antibody in rat spinal cord tissue for analysis by immunofluorescence. We noticed that the expression of F4/80, as well as the co-expression of PTEN and F4/80, was dramatically increased the spinal cords tissue (segments containing the lesion and 1 cm on each side of the lesion) (Fig. 1C, D). These data suggest that the expression of PTEN accumulates in macrophages after SCI.

2.2. Inhibition of PTEN activity promotes macrophage polarization to an M2 phenotype in vitro

To elucidate the role of PTEN in macrophages, we examined cultures of the mouse macrophage cell line RAW264.7. After knockdown of PTEN with small-interfering (si) RNA in RAW264.7 cells, cells were stimulated with LPS and IFN-γ. The expression levels of classically activated (M1) markers including TNF-alpha, CD16/32 and iNOS were detected via qPCR analysis. As shown in Fig. 2A, the relative mRNA expression levels of PTEN were decreased, and markers of M1 macrophage polarization were greatly minimized. Next, PTEN knockdown RAW264.7 cells were stimulated with IL-4 to polarize them towards an M2 phenotype. Using qPCR analysis, the expression levels of M2 markers Arg-1, CD206, Fizz1, and Ym1 were found to be dramatically increased (Fig. 2B). Additionally, immunoblot analysis confirmed the expression levels of PTEN, IL-10 and iNOS were decreased, while Arg-1 and CD206 levels were increased in RAW264.7 cells with PTEN knockdown (Fig. 2C). Moreover, the expression of M1 markers increased and M2 markers were decreased in cells with overexpression of PTEN via western blot analysis (Fig. 2D). In conclusion, knockdown of PTEN in macrophages promoted M2 polarization, while inhibiting M1 polarization *in vitro*, and overexpression of PTEN showed a contrary effect on M1/M2 polarization. Next, the cultured RAW264.7 cells were treated with bpV(pic), an inhibitor of PTEN activity. The expression of phospho-PTEN gradually decreased as the treatment dose of bpV(pic) increased (0, 10, and 20 nM). A marker of M1 macrophages, iNOS, was also diminished, while a marker of M2 macrophages, Arg-1, was increased. These results suggested that bpV(pic) treatment increased the M2/M1 ratio via the inhibition of PTEN activity in macrophages *in vitro* (Fig. 2E).

2.3. Inhibition of PTEN with bpV(pic) improves functional recovery after SCI

As previously reported, we generated ASC scaffolds from the spinal cords of normal rats, and combined the ASC scaffold with bpV(pic) (Tang et al., 2019). We then grafted either ASCs alone, bpV(pic) alone, or ASCs combined with bpV(pic) into rats receiving SCI surgery. The bpV(pic) and ASC combined with bpV(pic) conditions resulted in decreased motor neuron loss in comparison to control or ASC-only grafted

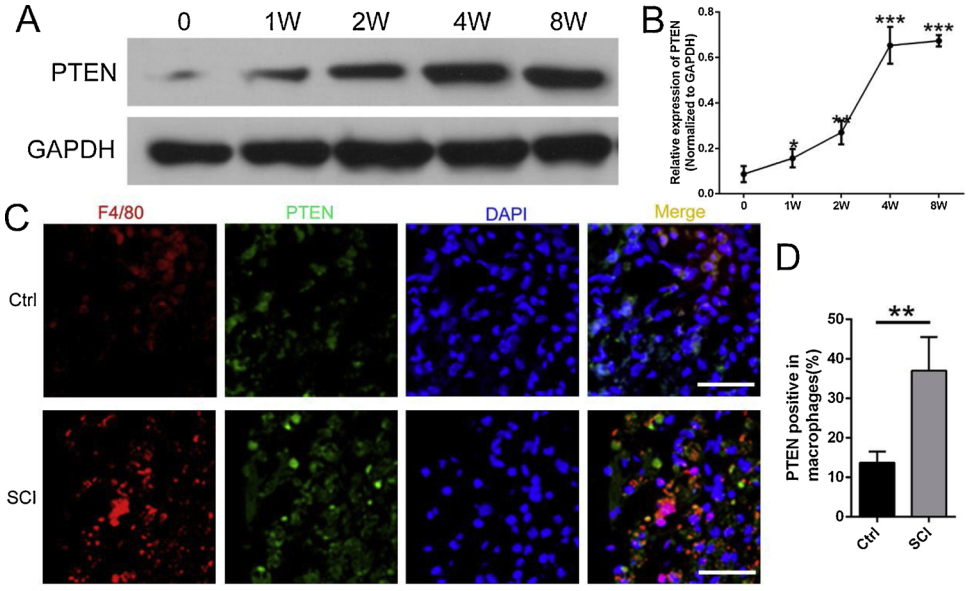

Fig. 1. PTEN expression accumulates in macrophages after SCI. A. Immunoblot analysis of PTEN and GAPDH levels in spinal cord tissue from rats at 0, 1, 2, 4, 8 weeks post SCI. (n = 3 independent experiments). B. Quantification of the PTEN expression from rats at 0, 1, 2, 4, 8 weeks post SCI in A. (n = 3 independent experiments). C. Representative confocal immunofluorescence images of F4/80 (red) and PTEN (green) in spinal cords from control and SCI rats. (n = 3: tissues were acquired from 3 different animals). Scale bar = 50 μm. D. Quantification of the PTEN and F4/80 double positive macrophages in B. (n = 3). *p < 0.05, **p < 0.01, ***p < 0.001; all data are shown as the mean ± SD.

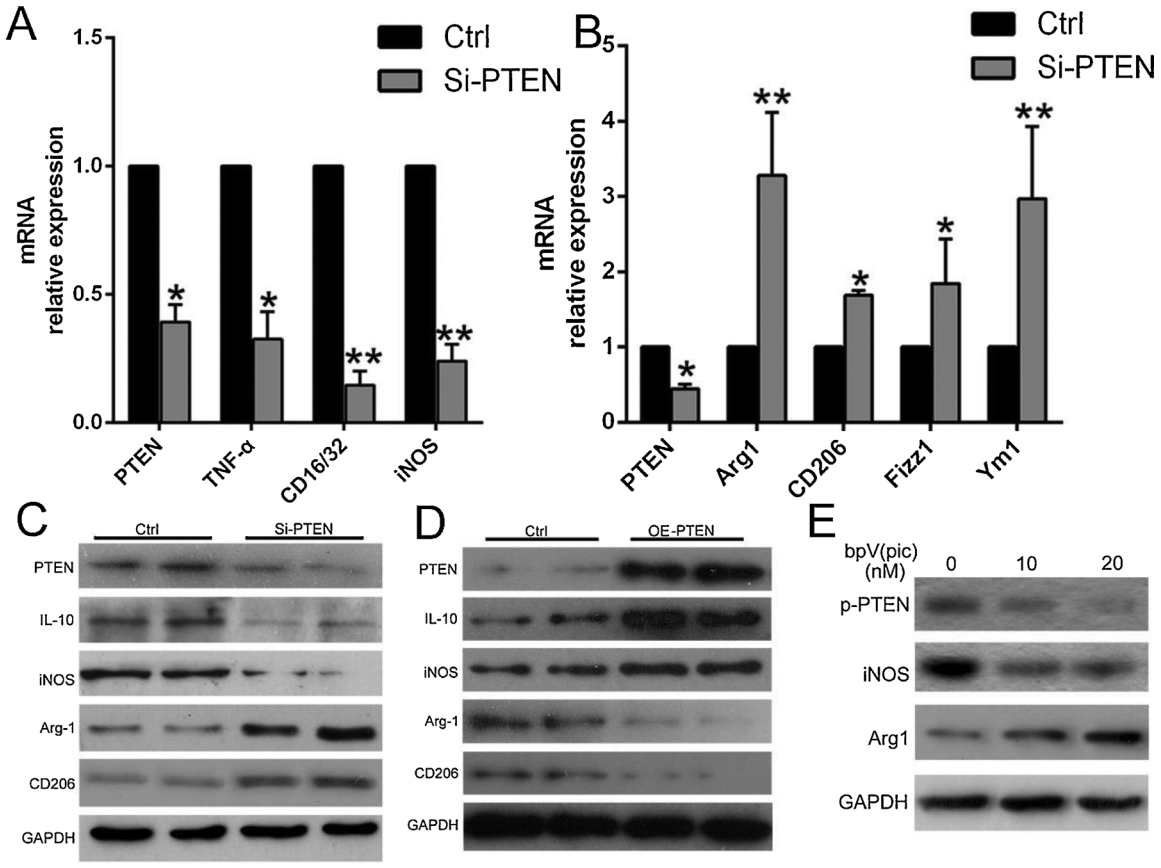

Fig. 2. Knockdown of PTEN or treatment with bpV(pic) promotes M2 macrophage polarization and decreases M1 polarization in RAW264.7 cells. A. RAW264.7 cells were treated with small interfering RNA against PTEN and then stimulated with LPS and IFN-γ; displayed are the relative mRNA levels of PTEN and the markers of M1 macrophages (TNF-a, CD16/32 and iNOS). (n = 3 independent experiments). B. RAW264.7 cells treated with small interfering RNA against PTEN and then stimulated with IL-4; displayed are the relative mRNA levels of PTEN and the markers of M2 macrophages (Arg-1, CD206, Fizz1, and Ym1). (n = 3 independent experiments). C. Immunoblot analysis of PTEN, IL-10, iNOS, Arg-1, CD206and GAPDH in RAW264.7 cells with PTEN knockdown and LPS plus IFN-γ stimulation. (n = 3 independent experiments). D. Immunoblot analysis of PTEN, IL-10, iNOS, Arg-1, CD206 and GAPDH in RAW264.7 cells with PTEN overexpression and IL-4 stimulation. (n = 3 independent experiments). E. Immunoblot analysis of p-PTEN, iNOS, and Arg-1 in RAW264.7 cells after treatment with different concentrations (0, 10, 20 nM) of bpV(pic). (n = 3 independent experiments). *$p < 0.05$, **$p < 0.01$; all data are shown as the mean ± SD.

spinal cords (Fig. 3A and B). H&E staining also revealed that the bpV (pic) and ASC combined with bpV(pic) groups displayed a diminished injury than the other two groups (Fig. 3C). In order to assess functional recovery, BBB scores were assessed (The BBB scores of the rats in all group were 21 at 1 day before SCI surgery), as shown in Fig. 3D, from 1 day to 12 weeks post-surgery. The bpV(pic) and ASC combined with bpV(pic) groups showed higher BBB scores compared to the control and ASC-only groups, with the ASC combined with bpV(pic) group displaying the highest level of functional recovery after SCI. We then assessed the cell proliferation in the Spinal cords from all groups with IHC of Ki67. The expression of Ki67 was enhanced in the bpV(pic) and ASC combined with bpV(pic) groups compared to control or ASC group (Fig. 3E and F). We also detected the expression of glial marker (GFAP, Fig. 3G and H) and neuronal marker (β-III-tubulin, Fig. 3I and *J*) in the Spinal cords from all groups. As expected, the expressions of GFAP and β-III-tubulin were also increased in the bpV(pic) and ASC combined with bpV(pic) groups compared to control or ASC group. Afterall, these data suggest that inhibition of PTEN with bpV(pic) promoted glial scar formation, but also promoted the axonal outgrowth, improved tissue sparing and locomotor function after SCI.

2.4. Treatment with bpV(pic) after SCI promotes macrophage polarization towards an M2 phenotype and inhibits polarization towards an M1 phenotype at the site of injury

To fully investigate the underlying mechanisms by which bpV(pic) was able to promote functional recovery after SCI, we examined changes in the expression of M1 and M2 markers in the spinal cord after SCI. As expected, F4/80 positive cells showed increased CD206 expression in the bpV(pic) and ASC plus bpV(pic) groups, as assessed by immunofluorescence staining analysed by confocal microscopy (Fig. 4A and B). Immunofluorescence analysis using an Arg-1 antibody showed similar results; the expression of Arg-1 was increased in the bpV(pic) and ASC plus bpV(pic) groups (Fig. 4C and D). Furthermore, we detected an increase in M2 marker expression with qPCR analysis. Following SCI, the expression levels of IL-10, Fizz1, and Ym1 were elevated in the bpV(pic) and ASC plus bpV(pic) groups (Fig. 4E–G). We examined M1 markers in the same way; in bpV(pic) and ASC plus bpV (pic) groups, immunofluorescence staining analysed by confocal microscopy revealed a reduction of iNOS expression in F4/80 positive macrophages after SCI (Fig. 5A and B), as well as a lower level of TNF-a (Fig. 5C and D). The mRNA levels of IL-6, TNF-a, and iNOS were confirmed to be reduced in the bpV(pic) and ASC plus bpV(pic) groups (Fig. 5E–G). These results indicated that *in vivo* treatment with bpV(pic) promoted the M2 phenotype and inhibited M1 polarization in macrophages after SCI.

3. Discussion

Inflammation is a prominent mediator of secondary damage in the CNS following injury(Guerrero et al., 2012; Yang et al., 2017). In the current study, we showed that the inhibition of PTEN played a crucial

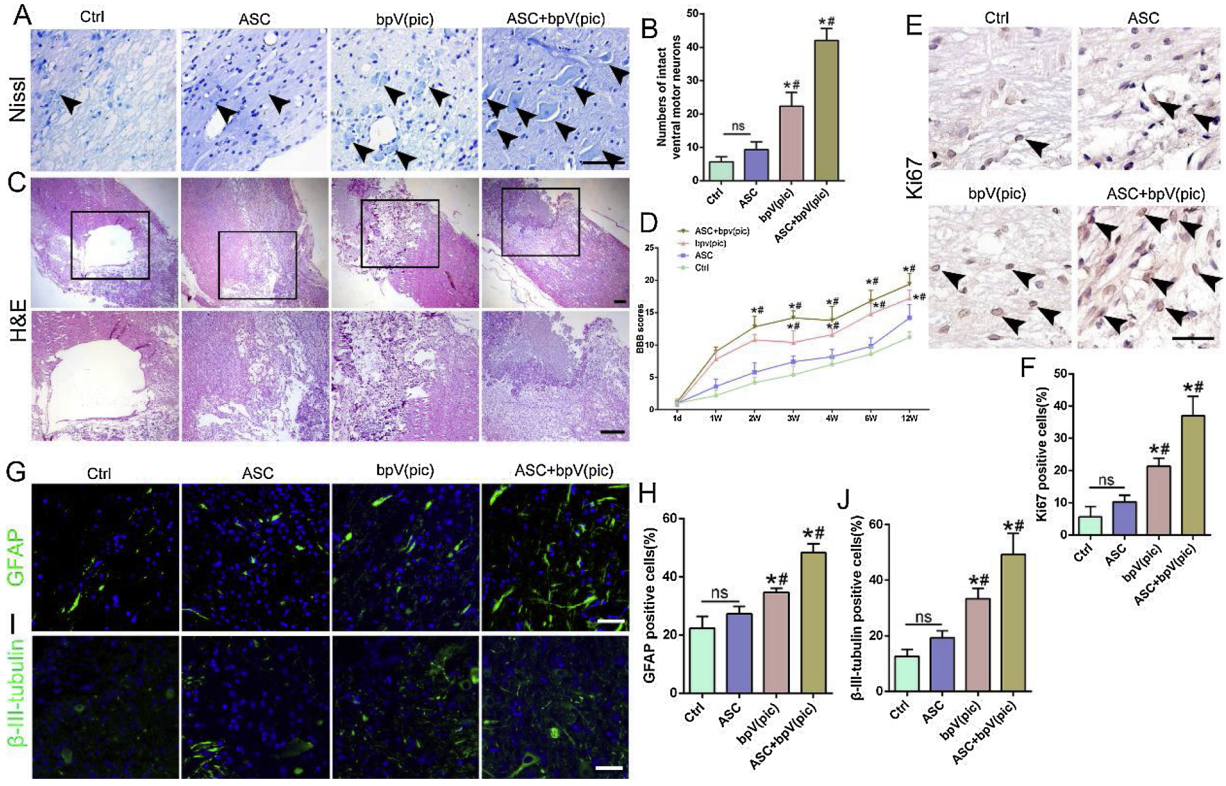

Fig. 3. BpV(pic) and ASC combined with bpV(pic) improves functional recovery after SCI. A. Nissl staining of motor neurons in the large anterior horn in different transplantation groups, 4 weeks post-SCI. Arrows are pointing to the cell bodies of the neurons. (n = 5); scale bar = 50 μm. B. Counts of the numbers of motor neurons in the anterior horn of the spinal cord. (n = 5). C. Representative H&E staining of spinal cords from different groups at 4 weeks post-SCI. (n = 5); scale bar = 50 μm. D. Plot of BBB locomotor scores of the different transplantation groups at different time points (from 1 day to 12 weeks) post-SCI. (n = 5). E. Representative immunohistochemistry images of Ki67 in spinal cords from different groups at 4 weeks post-SCI. (n = 5); scale bar = 50 μm. Arrows are pointing to the positive cells. F. Quantification of the Ki67 positive cells in E. (n = 5). G. Representative immunofluorescence images of GFAP (green) in spinal cords from different groups of rats at 4 weeks post-SCI. (n = 5); scale bar = 50 μm. H. Quantification of the GFAP positive cells in G. (n = 5). I. Representative immunofluorescence images of β-III-tubulin (green) in spinal cords from different groups of rats at 4 weeks post-SCI. (n = 5); scale bar = 50 μm. *J*. Quantification of the β-III-tubulin positive cells in G. (n = 5). * means $P < 0.05$ compared to the control group; # means $P < 0.05$ compared to the ASC group; ns = not significant. All data are shown as the mean ± SD.

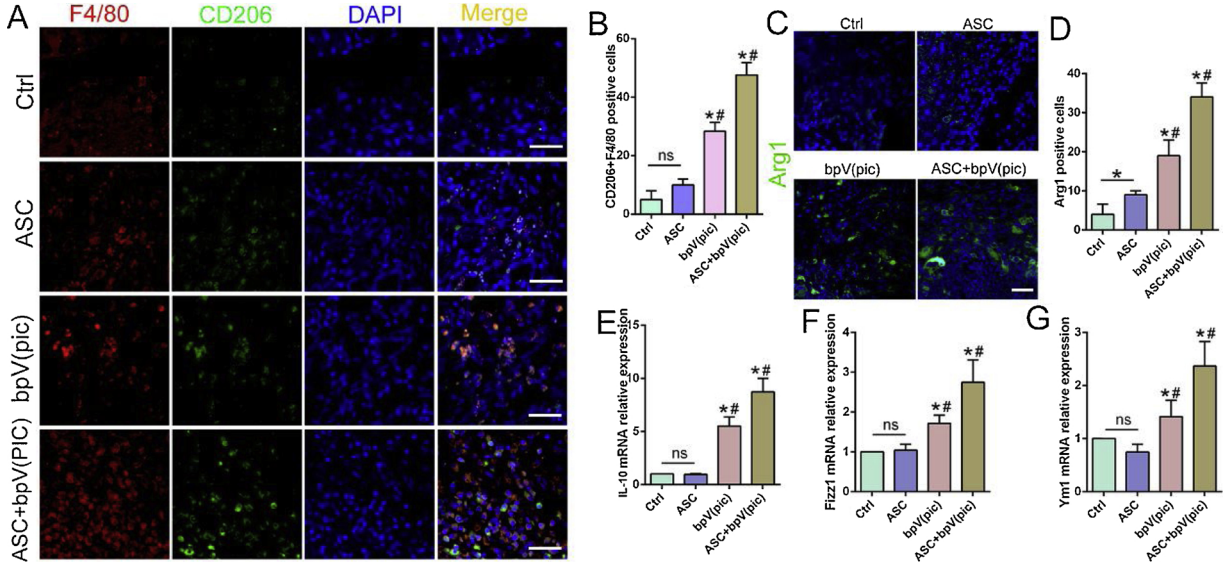

Fig. 4. BpV(pic) and ASC combined with bpV(pic) promotes M2 macrophage polarization in the injury site after SCI. A. Representative confocal immunofluorescence images of F4/80 (red) and CD206 (green) in spinal cords from different groups of rats at 4 weeks post-SCI. (n = 5); scale bar = 50 μm. B. Quantification of the CD206 expression in F4/80 positive macrophages in a. (n = 5). C. Representative immunofluorescence images of Arg-1 in spinal cords from different groups of rats at 4 weeks post-SCI. (n = 5). Scale bar = 50 μm. D. Quantification of the Arg-1 expression in c. (n = 5). E. Relative mRNA levels of IL-10, Fizz1 (F), and Ym1 (G) in spinal cords from different groups of rats at 4 weeks post-SCI. (n = 5). *means $P < 0.05$ compared to the control group; # means $P < 0.05$ compared to the ASC group; ns = not significant. All data are shown as the mean ± SD.

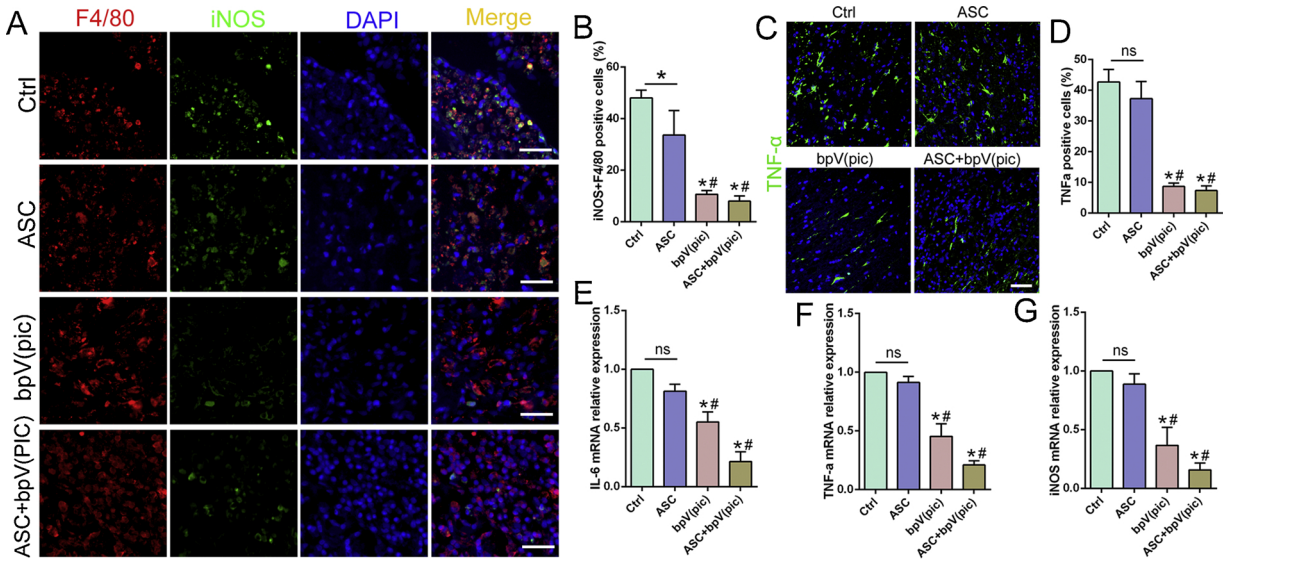

Fig. 5. BpV(pic) and ASC combined with bpV(pic) decreases M1 polarization in the injury site after SCI. A. Representative confocal immunofluorescence images of F4/80 (red) and iNOS (green) in spinal cords from different groups of rats at 4 weeks post-SCI. (n = 5); scale bar = 50 μm. B. Quantification of the iNOS expression in F4/80 positive macrophages in a. (n = 5). C. Representative immunofluorescence images of TNF-α in the spinal cords from different groups of rats at 4 weeks post-SCI. (n = 5). Scale bar = 50 μm. D. Quantification of the TNF-α expression in c. (n = 5). E. Relative mRNA levels of IL-6, TNF-a (F), and iNOS (G) in the spinal cords from different groups of rats at 4 weeks post-SCI. (n = 5). *means $P < 0.05$ compared to the control group; # means $P < 0.05$ compared to the ASC group; ns = not significant. All data are shown as the mean ± SD.

role in regulating M2 macrophage activation and improving locomotor recovery after SCI in rats. The expression level of PTEN was significantly increased in macrophages after SCI. In cultured macrophages, knockdown of PTEN or treatment with bpV(pic) to inhibit the phosphorylation of PTEN promoted M2 polarization and decreased M1 polarization. *in vivo*, bpV(pic) treatment enhanced the cell proliferation, promoted M2 macrophage activation, increased the abundance of M2-type macrophages at the injury site, axonal outgrowth to the lesion cavity, and improved tissue sparing and locomotor function after SCI. Furthermore, combining bpV(pic) with ASC scaffolds made from the spinal cord of rats enhanced the effect of bpV(pic) on promoting M2 polarization. Our studies suggested that PTEN may be a regulator of the polarization of M1/2 macrophages, and thus targeting PTEN may be a potential therapeutic target for the promotion of neurological recovery after SCI.

Previous studies have revealed that macrophages possess a high degree of plasticity, with the ability to quickly adjust in response to CNS damage(Gensel et al., 2009; Laskin, 2009). It has also been suggested that alternatively-activated macrophages are involved in recovery following SCI(Hausmann, 2003). In our study, M2-type macrophages were increased following knockdown of PTEN or by inhibition of PTEN activity with bpV(pic). Other studies have reported that classically activated macrophages, producing pro-inflammatory cytokines and oxidative metabolites, are predominant at the site of injury and surrounding tissue after SCI(Novak and Koh, 2013). Following the inhibition of PTEN expression or PTEN activity, M1 related pro-inflammatory cytokines (such as IL-6) were diminished, resulting in an obstruction of the secondary injury process. Using immunofluorescence labeling of specific markers (such as CD206 and Arg-1), we confirmed that M2-type macrophages were elevated at the injury site after SCI. As has been reported in other studies, an elevation of M2-type macrophages in the injury site promoted axonal outgrowth to the lesion cavity, tissue sparing, and functional recovery from SCI(Ma et al., 2015). We also noticed that the expression of glial marker GFAP increased after bpV (pic) treatment, which means inhibition of PTEN would promote glial scar formation in SCI. All in all, we speculate that the effect of bpV(pic) on macrophages exert dominant effect in the neuronal recovery after SCI.

While our findings were in agreement with previous reports(Liu et al., 2019), more interestingly, we showed that an ASC combined with bpV(pic) had an enhanced effect on promoting M2 polarization. In our previous studies, ASC scaffolds, seeded with human umbilical cord blood-derived mesenchymal stem cells, were able to bridge a spinal cord cavity and promote long-distance axonal regeneration and functional recovery following SCI in rats(Liu et al., 2013). Here, we showed an enhanced effect of an ASC scaffold upon combination with bpV(pic), the inhibitor of PTEN activity. We speculate that this was due to the fact that the ASC scaffold was made using spinal cords from the same species used in the study. The ASC material therefore had perfect biomimetic properties, and was likely able to recruit more macrophages to the injury site. Furthermore, when an ASC was combined with the effect of the PTEN inhibitor bpV(pic), M2 polarization was able to be greatly enhanced. We believe that macrophage polarization is only one possible mechanism for the observed neuroprotective effect of bpV(pic) in combination with an ASC scaffold after SCI. Further studies are thus needed in order to uncover the precise mechanism of action of PTEN in the regulation of macrophage polarization.

In the present study, we found that the expression of PTEN significantly increased in macrophages following SCI. We then used the inhibitor of PTEN, bpV(pic), and ASCs combined with bpV(pic) to treat SCI in rats. Functional recovery was greatly improved and damage to the spinal cord tissue was ameliorated, with an accumulation of M2-type macrophages observed at the injury site. These results suggest that inhibiting PTEN promotes the M2 polarization of macrophages, resulting in improved functional recovery following SCI.

4. Methods and materials

4.1. Acute spinal cord injury model and graft transplantation

Adult male Sprague-Dawley rats (250–300 g) were purchased from the animal center of Youjiang Medical College for Nationalities. All animals were housed in standard temperature conditions with a 12 h light/dark cycle and regularly fed with food and water. All surgical procedures were performed under anesthesia by intraperitoneal injection with 10% chloral hydrate (0.4 ml/100 g). The skin was incised to

expose the vertebral column and to perform a laminectomy at the T9 level. Under a surgical microscope, two right-sided hemisections of the spinal cord were created using a microdissection scissor at levels T9 and T10. Animals that underwent laminectomy without SCI were used as a sham control (n = 4). Animals with a hemisected SCI were randomly divided into four groups and received the graft transplantation at 1 day post-surgery: animals treated with an ASC scaffold implantation (n = 6), animals treated with bpV(pic) (100 mg/kg) implantation (n = 6), animals treated with the implantation of an ASC scaffold with bpV(pic) (100 mg/kg) (n = 6), and SCI only (control, n = 6). To prevent infection, rats were treated with ampicillin (100 mg/kg) and gentamicin (12 mg/kg) subcutaneously once a day following surgery for 3 days. Manual bladder expression was performed twice a day until they regained bladder control, approximately 3 to 5 days after initial injury. All animal experiments were approved by the local ethics committee for animal research at Youjiang Medical College for Nationalities, and were performed in accordance with international standards for animal welfare.

4.2. ASC scaffold preparation

Adult Sprague Dawley (SD) rats were sacrificed by intraperitoneal injection with 10% chloral hydrate (60 ml/kg). The thoracic spinal cords were harvested. The chemical extraction for ASC preparation was based on a previously described procedure(Tang et al., 2019). Briefly, thoracic spinal cords were treated with a series of detergents including distilled water, Triton X-100 and sodium deoxycholate solution. All samples were subsequently freeze-dried for 24 h in a freeze dryer and sterilized by irradiation (3 kGy) with Cobalt-60 gamma rays before being used.

4.3. Locomotion recovery assessment

Motor function recovery was assessed using the Basso, Beattie, and Bresnahan (BBB) locomotor rating scale. Individual rats were placed on an open field and observed for 4 min by two observers blind to the treatment condition. A score of 0 indicates complete immobility, and a score of 21 indicates normal function. The scores were graded according to the rat's motor motion and rating scale. The test was carried out once a week after transplantation up to 12 weeks post-surgery.

4.4. In vitro experiments

The RAW264.7 cell line (TIB-71) (ATCC, Manassas, VA, USA) was cultured in Dulbecco's Modified Eagle Medium (DMEM) containing 10% fetal bovine serum (Gibco, Carlsbad, CA, USA). For M1 or M2 polarization, cultured Raw264.7 cells were incubated with IFN-γ (20 ng/mL) and LPS (100 ng/mL) for 6 h or with IL-4 (20 ng/mL) for 48 h. For the knockdown of PTEN expression, we transiently transfected cells with siRNA using Lipofectamine RNAi MAX (Invitrogen, Carlsbad, CA, USA) in Opti-MEM medium (Invitrogen), according to the manufacturer's instructions. The sequences of SiRNA used in this study were as follows: PTEN, sense: 5′-CGUGUACUACCUCAUGAGCUU-3′, antisense: 5′-GCGCAGAUACGUUCAUAGCUU-3′; Non-specific siRNA sequences were used as negative controls, sense: 5′-UUCUCCGAACGUG UCACG UTT-3′, and antisense: 5′-ACGUGACACGUUCGGAGAATT-3′. The efficiency of transfection was measured by western blot and qRT-PCR.

4.5. Western blot analysis

Animals were deeply anesthetized with an overdose of chloral hydrate, the spinal cords tissue segments containing the lesion (1 cm on each side of the lesion) was quickly removed, put on ice, frozen in liquid nitrogen, and kept at −80 °C until use. Tissues and cells were lysed using lysis buffer (62.5 mM Tris−HCl [pH 6.8], 10% glycerol, 2% SDS, 50 mM dithiothreitol, and 0.01% bromophenol blue at 96 °C for 10 min. The samples were separated with SDS-PAGE for 70 min, and after electrophoresis, proteins were transferred onto membranes (Bio-Rad Laboratories, USA) using a wet transfer method. Each membrane was then incubated in primary antibodies overnight at 4 °C on a shaker. After incubation in specific secondary antibodies, immunoblots were detected using an enhanced chemiluminescence kit (ECL kit, proteintech, USA).

4.6. Immunofluorescence analysis

10 μm frozen spinal cord tissue sections were rewarmed at room temperature for 30 min and blocked with sheep serum working solution at room temperature for 2 h. The tissues were incubated in primary antibodies overnight at 4 °C. The sections were subsequently washed 3 times and incubated in the corresponding fluorescent secondary antibodies (Goat anti-rabbit 594 and Goat anti-mouse FITC, 1:500, Thermo Fisher Scientific, Waltham, MA, USA) for 1 h at room temperature. The sections were then stained with DAPI, and observed by fluorescent microscopy (Olympus, Japan). The percentages of the double positive cells were quantified in at least three versions from three different slices.

4.7. Antibodies

Anti-p-PTEN (#9554, Cell Signaling Technology, USA), anti-PTEN (#9188, Cell Signaling Technology, USA), anti-F4/80 (ab6640, abcam, USA), anti-GFAP (#3670, Cell Signaling Technology, USA), anti-beta-III-tubulin (#5568, Cell Signaling Technology, USA), anti-IL-10 (60269-1-Ig, proteintech, USA), anti-iNOS (ab15323, abcam, USA), anti-TNF-a (GTX110520, Genetex, USA), anti-Arg-1 (#93668, Cell Signaling Technology, USA), anti-CD206 (ab64693, abcam, USA), anti-GAPDH (AC033, abclonal, China).

4.8. Nissl staining

Sections were rewarmed at room temperature for 30 min, then immersed in 100% ethanol, 75% ethanol, and distilled water for 30 s each, then stained with a 0.1% cresyl violet solution at 37 °C for 5 min. The sections were washed in distilled water, immersed in 95% ethanol for 30 s, and soaked in anhydrous ethanol, anhydrous ethanol, and xylene for 5 min each. The sections were sealed with neutral gum and observed under a microscope.

4.9. Quantitative RT-PCR

Total RNA was isolated with Trizol (Life Technologies, USA) and reverse transcription was performed with reverse transcriptase (Takara Bio, Japan) according to the manufacturer's instructions. RT-PCR was performed using multiple kits (SYBR Premix Ex TAQ, Takara Bio, Japan) according to the manufacturer's instructions. To determine the expression of mRNA, each gene was normalized to the expression level of the housekeeping gene GAPDH. The primers used in the present study are listed below: Arg-1, forward: ACCTGGCCTTTGTT GATGTCC CTA, reverse: AGAGATGCTTCCAACTGCCAGACT; CD206, forward: TTGG ACGGATAGATGGAGGG, reverse: CCAGGCAGTTGAG GAGGTTC; TNF-a up: CTCAAGCCCTGGTATGAGCC, down: GGCTGGGTAGAGAAC GGATG; iNOS up: TTGCTTCTGTGCTAATGCGG, down: AAGGCGTAGC TGAACAAGGA; IL-10 up: CAGTCAGCCAGACCCACA, down: GGCAAC CCAAGTAACCCT; IL-6 up: TCCTACCCC AACTTCCAATGC, down: TAG CACACTAGGTTTGCCGAG; Ym1, forward, AGAAGG GAGTTTCAAA CCT, reverse, GTCTTGCTCATGTGTGTAAGTGA; Fizz-1, forward: TCCA GCTGATGGTCCCAGTGAATA, reverse: ACAAGCACACCCAGTAGCA GTCAT; GAPDH, forward: TCAACGACCCCTTCATTGAC, reverse: ATG CAGGGATGAT GTTCTGG;

4.10. Statistical analysis

All experiments were performed at least three times. All data were presented as the mean ± standard deviation (SD) using SPSS version 20.0 software for statistical analysis, with graphs generated in GraphPad Prism 6.0. The student's *t*-test was used to assess statistically significant differences in the data between groups. A p-value of less than 0.05 was considered statistically significant. Statistical significance indicated as ns for not significant; * or # for $P < 0.05$; ** for $P < 0.01$; *** for $P < 0.001$;

Authors contribution

Y.J.T. conceived the project, designed and supervised the experiments. Q.S.L. wrote the manuscript. K.L. and J.L. performed the experiments and analyzed the data. C.L.Y., T.S. and J.H.W. helped with the animal experiments. J.H.W. and K.Y.X. helped prepare the figures and finished the IHC/IF and WB analysis.

Declaration of Competing Interest

The authors declare that we have no conflict of interest.

Acknowledgments

Funding: This work was supported by the National Natural Science Foundation of China (approval number: 81560213 and 81760450) and supported by Natural Science Foundation of Guangxi (approval number: 2018GXNSFAA138074).

References

Allison, D.J., Ditor, D.S., 2015. Immune dysfunction and chronic inflammation following spinal cord injury. Spinal Cord 53, 14–18.
Benoit, M., Desnues, B., Mege, J.L., 2008. Macrophage polarization in bacterial infections. J. Immunol. 181, 3733–3739.
Burns, A.S., Marino, R.J., Kalsi-Ryan, S., Middleton, J.W., Tetreault, L.A., Dettori, J.R., Mihalovich, K.E., Fehlings, M.G., 2017. Type and timing of rehabilitation following acute and subacute spinal cord injury: a systematic review. Global Spine J. 7, 175S–194S.
Cambier, C.J., Takaki, K.K., Larson, R.P., Hernandez, R.E., Tobin, D.M., Urdahl, K.B., Cosma, C.L., Ramakrishnan, L., 2014. Mycobacteria manipulate macrophage recruitment through coordinated use of membrane lipids. Nature 505, 218–222.
David, S., Kroner, A., 2011. Repertoire of microglial and macrophage responses after spinal cord injury. Nat. Rev. Neurosci. 12, 388–399.
Ding, N., Wang, Y., Dou, C., Liu, F., Guan, G., Wei, K., Yang, J., Yang, M., Tan, J., Zeng, W., Zhu, C., 2019. Physalin D regulates macrophage M1/M2 polarization via the STAT1/6 pathway. J. Cell. Physiol. 234, 8788–8796.
Fawcett, J.W., Curt, A., Steeves, J.D., Coleman, W.P., Tuszynski, M.H., Lammertse, D., Bartlett, P.F., Blight, A.R., Dietz, V., Ditunno, J., Dobkin, B.H., Havton, L.A., Ellaway, P.H., Fehlings, M.G., Privat, A., Grossman, R., Guest, J.D., Kleitman, N., Nakamura, M., Gaviria, M., Short, D., 2007. Guidelines for the conduct of clinical trials for spinal cord injury as developed by the ICCP panel: spontaneous recovery after spinal cord injury and statistical power needed for therapeutic clinical trials. Spinal Cord 45, 190–205.
Fleming, J.C., Norenberg, M.D., Ramsay, D.A., Dekaban, G.A., Marcillo, A.E., Saenz, A.D., Pasquale-Styles, M., Dietrich, W.D., Weaver, L.C., 2006. The cellular inflammatory response in human spinal cords after injury. Brain 129, 3249–3269.
Franken, L., Schiwon, M., Kurts, C., 2016. Macrophages: sentinels and regulators of the immune system. Cell. Microbiol. 18, 475–487.
Gensel, J.C., Nakamura, S., Guan, Z., van Rooijen, N., Ankeny, D.P., Popovich, P.G., 2009. Macrophages promote axon regeneration with concurrent neurotoxicity. J. Neurosci. 29, 3956–3968.
Gensel, J.C., Zhang, B., 2015. Macrophage activation and its role in repair and pathology after spinal cord injury. Brain Res. 1619, 1–11.
Guerrero, A.R., Uchida, K., Nakajima, H., Watanabe, S., Nakamura, M., Johnson, W.E., Baba, H., 2012. Blockade of interleukin-6 signaling inhibits the classic pathway and promotes an alternative pathway of macrophage activation after spinal cord injury in mice. J. Neuroinflamm. 9, 40.
Halsey, A.M., Conner, A.C., Bill, R.M., Logan, A., Ahmed, Z., 2018. Aquaporins and their regulation after spinal cord injury. Cells 7.
Hausmann, O.N., 2003. Post-traumatic inflammation following spinal cord injury. Spinal Cord 41, 369–378.
Ji, X.C., Dang, Y.Y., Gao, H.Y., Wang, Z.T., Gao, M., Yang, Y., Zhang, H.T., Xu, R.X., 2015. Local injection of Lenti-BDNF at the lesion site promotes M2 macrophage polarization and inhibits inflammatory response after spinal cord injury in mice. Cell. Mol. Neurobiol. 35, 881–890.
Kigerl, K.A., Gensel, J.C., Ankeny, D.P., Alexander, J.K., Donnelly, D.J., Popovich, P.G., 2009. Identification of two distinct macrophage subsets with divergent effects causing either neurotoxicity or regeneration in the injured mouse spinal cord. J. Neurosci. 29, 13435–13444.
Kirshblum, S.C., Burns, S.P., Biering-Sorensen, F., Donovan, W., Graves, D.E., Jha, A., Johansen, M., Jones, L., Krassioukov, A., Mulcahey, M.J., Schmidt-Read, M., Waring, W., 2011. International standards for neurological classification of spinal cord injury (revised 2011). J. Spinal Cord Med. 34, 535–546.
Kong, X., Gao, J., 2017. Macrophage polarization: a key event in the secondary phase of acute spinal cord injury. J. Cell. Mol. Med. 21, 941–954.
Laskin, D.L., 2009. Macrophages and inflammatory mediators in chemical toxicity: a battle of forces. Chem. Res. Toxicol. 22, 1376–1385.
Li, F., Cheng, B., Cheng, J., Wang, D., Li, H., He, X., 2015. CCR5 blockade promotes M2 macrophage activation and improves locomotor recovery after spinal cord injury in mice. Inflammation 38, 126–133.
Li, J., Liu, Y., Xu, H., Fu, Q., 2016. Nanoparticle-delivered IRF5 siRNA facilitates M1 to M2 transition, reduces demyelination and neurofilament loss, and promotes functional recovery after spinal cord injury in mice. Inflammation 39, 1704–1717.
Liu, G., Yang, H., 2013. Modulation of macrophage activation and programming in immunity. J. Cell. Physiol. 228, 502–512.
Liu, J., Chen, J., Liu, B., Yang, C., Xie, D., Zheng, X., Xu, S., Chen, T., Wang, L., Zhang, Z., Bai, X., Jin, D., 2013. Acellular spinal cord scaffold seeded with mesenchymal stem cells promotes long-distance axon regeneration and functional recovery in spinal cord injured rats. J. Neurol. Sci. 325, 127–136.
Liu, R., Liao, X.Y., Tang, J.C., Pan, M.X., Chen, S.F., Lu, P.X., Lu, L.J., Zhang, Z.F., Zou, Y.Y., Bu, L.H., Qin, X.P., Wan, Q., 2019. BpV(pic) confers neuroprotection by inhibiting M1 microglial polarization and MCP-1 expression in rat traumatic brain injury. Mol. Immunol. 112, 30–39.
Ma, S.F., Chen, Y.J., Zhang, J.X., Shen, L., Wang, R., Zhou, J.S., Hu, J.G., Lu, H.Z., 2015. Adoptive transfer of M2 macrophages promotes locomotor recovery in adult rats after spinal cord injury. Brain Behav. Immun. 45, 157–170.
Mosser, D.M., Edwards, J.P., 2008. Exploring the full spectrum of macrophage activation. Nature reviews. Immunology 8, 958–969.
Novak, M.L., Koh, T.J., 2013. Phenotypic transitions of macrophages orchestrate tissue repair. Am. J. Pathol. 183, 1352–1363.
Pieters, J., 2008. Mycobacterium tuberculosis and the macrophage: maintaining a balance. Cell Host Microbe 3, 399–407.
Shapouri-Moghaddam, A., Mohammadian, S., Vazini, H., Taghadosi, M., Esmaeili, S.A., Mardani, F., Seifi, B., Mohammadi, A., Afshari, J.T., Sahebkar, A., 2018. Macrophage plasticity, polarization, and function in health and disease. J. Cell. Physiol. 233, 6425–6440.
Shechter, R., London, A., Varol, C., Raposo, C., Cusimano, M., Yovel, G., Rolls, A., Mack, M., Pluchino, S., Martino, G., Jung, S., Schwartz, M., 2009. Infiltrating blood-derived macrophages are vital cells playing an anti-inflammatory role in recovery from spinal cord injury in mice. PLoS Med. 6, e1000113.
Stout, R.D., Suttles, J., 2004. Functional plasticity of macrophages: reversible adaptation to changing microenvironments. J. Leukoc. Biol. 76, 509–513.
Tang, Y.J., Li, K., Yang, C.L., Huang, K., Zhou, J., Shi, Y., Xie, K.G., Liu, J., 2019. Bisperoxovanadium protects against spinal cord injury by regulating autophagy via activation of ERK1/2 signaling. Drug Des. Devel. Ther. 13, 513–521.
Wang, X., Cao, K., Sun, X., Chen, Y., Duan, Z., Sun, L., Guo, L., Bai, P., Sun, D., Fan, J., He, X., Young, W., Ren, Y., 2015. Macrophages in spinal cord injury: phenotypic and functional change from exposure to myelin debris. Glia 63, 635–651.
Yang, Y., Guo, C., Liao, B., Cao, J., Liang, C., He, X., 2017. BAMBI inhibits inflammation through the activation of autophagy in experimental spinal cord injury. Int. J. Mol. Med. 39, 423–429.
Yao, A., Liu, F., Chen, K., Tang, L., Liu, L., Zhang, K., Yu, C., Bian, G., Guo, H., Zheng, J., Cheng, P., Ju, G., Wang, J., 2014. Programmed death 1 deficiency induces the polarization of macrophages/microglia to the M1 phenotype after spinal cord injury in mice. Neurotherapeutics 11, 636–650.
Zhang, Z., Li, M., Wang, Y., Wu, J., Li, J., 2014. Higenamine promotes M2 macrophage activation and reduces Hmgb1 production through HO-1 induction in a murine model of spinal cord injury. Int. Immunopharmacol. 23, 681–687.